Geometrical Acceptances of CLAS for Exclusive Electroproduction of ρ^0 and ω Mesons at Large Q^2 Studied with FASTMC

S. Morrow, M. Guidal, C. Hadjidakis
IPN Orsay, F–91406, Orsay, France

D. Doré, L. Morand
SPhN, C.E.A. Saclay, F–91191 Gif–sur–Yvette, France

5th February 2001

Abstract

This report describes studies made of the acceptance of the CLAS detector for the exclusive electroproduction of ρ^0 and ω mesons, carried out principally using FASTMC. Studies have been made of the effect of moving the target, altering the strength of the magnetic field of the detector and of switching the polarity of the magnetic field.

1 Introduction

The main results of the simulations shown in this report were obtained with the FASTMC Monte–Carlo simulation program [1]. This Monte–Carlo has been used in conjunction with event generators for exclusive vector meson electroproduction (RHOCOL [2] for ρ^0 production and GENOVA [3] for ω production) on the nucleon, above the resonance region. The current study has been made for deeply virtual meson production (DVMP). It is motivated by a proposal [4] to measure the exclusive electroproduction of vector mesons, on the nucleon, at large Q^2, with the CLAS detector at CEBAF.

FASTMC takes into account the geometrical effects related to the CLAS detector and parameterises the bending of particles in the main toroidal magnetic field of the detector. It also includes resolution through smearing of the momentum and energy variables. This report presents a study of the geometrical acceptance of the CLAS detector for this specific reaction using FASTMC.

Unless otherwise stated, the parameters used to run all simulations were as follows. Electron beam energy E_0=5.75 GeV; Q^2>2 GeV^2; W>2 GeV and -t<1.5 GeV^2. The cross section for ρ^0 electroproduction, used by RHOCOL, is based on a Vector meson Dominance Model (VDM) parameterisation.

When demanding an accepted electron in the CLAS detector, the requirement has been made throughout that it be detected in the 3 drift chamber regions, the scintillation counters, the Cerenkov counters and the electromagnetic calorimeter. The electromagnetic calorimeter, which defines the angular acceptance for the scattered electrons in this experiment, covers the angular

range $8°<\theta<45°$. The angular acceptance for charged hadrons, defined by the drift chambers and scintillation counters, is $8°<\theta<142°$. Section 2 describes the results found, for the effect on the acceptances, of shifting the target position. In sections 3 and 4 the effect of varying the magnetic field strength and switching the magnetic field polarity are discussed, respectively. These sections all discuss the case for ρ^0 production only. In section 5 the results for ω production are presented. Finally, in section 6, a conclusion from the study is made.

2 Target Position

In order to investigate methods of increasing the available acceptance of the CLAS detector in the DVMP experiment, studies have been made with the target displaced from the nominal position. The possibility of moving the target upstream (along the electron beam line) has been tested. This was proposed as a means of increasing the geometrical acceptance since the reaction products are emitted mainly in a forward direction. Therefore it was thought that moving the target in this way might lower the minimum detection angle for the reaction products, and allow an increased number of particles to be detected.

A comparison of the results achieved by placing the target at the nominal position and at 1 m upstream of this position are shown, respectively, in figures 1 and 2. The integrated acceptances shown have been calculated as the percentage number of events, fulfilling certain coincidence criteria (given in the figure captions), over the total number of events generated.

The reaction of interest is

$$e^- + p \rightarrow e^- + p + \rho^0$$

where the ρ^0 subsequently decays into $\pi^+ + \pi^-$ in the time scale of $\simeq 10^{-24}$ s and so cannot be detected directly. The signature that this reaction has occurred, therefore, is the presence of a coincident e^-, p, π^+ and π^- combination in the detector. The detection of any 3 of these 4 particles is enough to fully determine the kinematics of the reaction. When this is done the missing mass technique is used to identify the fourth particle. As can be seen from both figures, the criterion which gives the highest acceptance for the experiment is $e^- + p + \pi^+$. The reason for this is that the π^-, due to its negative charge, is bent towards the beam axis and is lost in the forward 'hole' of the detector. It can be seen by comparing with figure 2 that the acceptance increases by a factor of $\sim$2 in all variables when the target is displaced from its nominal position.

In order to check the reliability of FASTMC, the results of a more thorough simulation, made using GSIM [5], are shown in figure 3 for the target in the nominal position. These plots may be compared with those obtained from FASTMC in figure 1. Some differences can be noted: for instance GSIM shows the acceptance extending to a higher Q^2 than FASTMC. Also the GSIM results show an acceptance which is in general $\sim$5 % higher for the criterion $e^- + p + \pi^+$ and 2–3 % lower for the criteria involving a detected π^- particle. Despite this, we consider the FASTMC results are in close enough agreement with those of

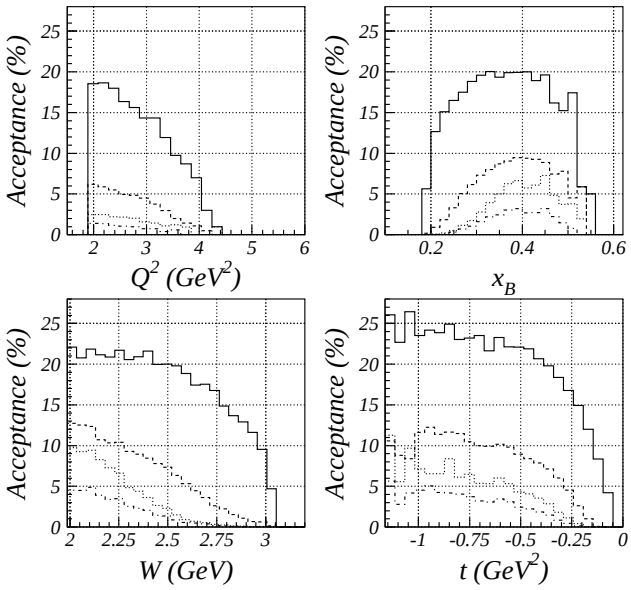

Figure 1: *The percentage of events accepted in CLAS for the kinematic variables Q^2, x_B, W and t. The target has been placed at the nominal position. The criteria used to define an event were: Full histogram $e^- + p + \pi^+$, Dashed histogram $e^- + p + \pi^-$, Dotted histogram $e^- + \pi^+ + \pi^-$ and Dot–Dashed histogram $e^- + p + \pi^+ + \pi^-$.*

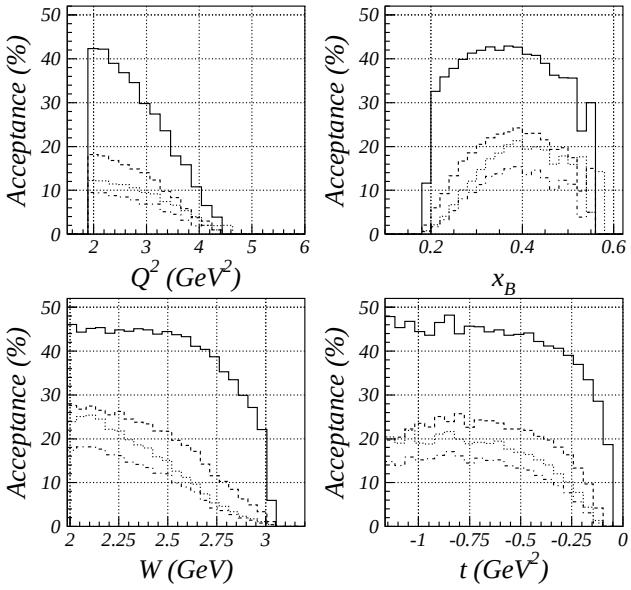

Figure 2: *As figure 1, with the target displaced upstream by 1 m.*

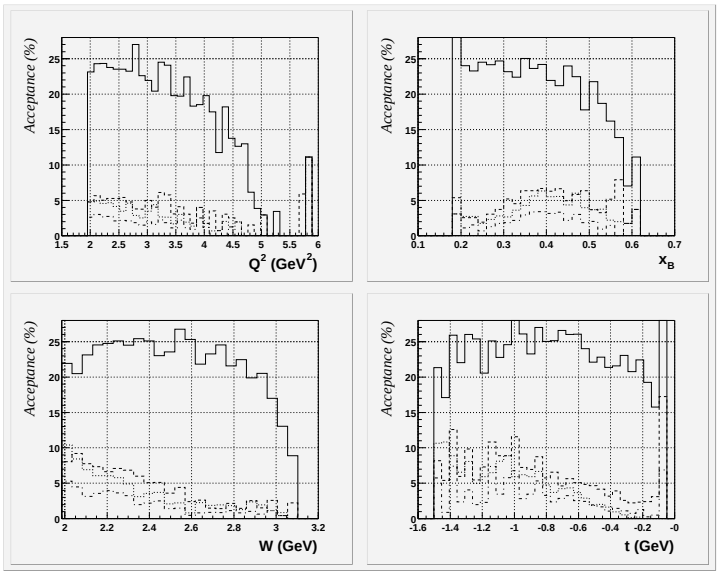

Figure 3: *As figure 1, results from GSIM simulations.*

GSIM for it to be trusted to give a broad overview of the most important effects on the geometrical acceptances. Results from FASTMC are more easily obtainable than from GSIM because of its higher execution speed, which made it suitable for this study, and because of the possibility of shifting the target position and still being able to reconstruct such events.

In passing we also note that the increase in acceptance seen at 5.75 GeV between figures 1 and 2, is also observed with a beam energy of 4 GeV, as shown in figures 4 and 5. Although the increase in acceptance observed here is less, around 50 %.

To understand what causes this increase in acceptance we first look at the scattered electron kinematics. The distribution of acceptance as a function of θ_e is shown in figure 6, for the target at 1, 0.5 and 0 m upstream of the nominal position. For comparison, the same distribution is shown in figure 7 for the result of a GSIM simulation with the target at nominal position only. The 2 simulations are in rough agreement. Figure 6 shows that the minimum electron scattering angle does not change with the target position. This can be understood in terms of the dependence of θ_e on Q^2 (see the inset of figure 6). The minimum θ_e is defined by the minimum Q^2. In this simulation only values of Q^2>2 GeV^2 were considered (since this is the region of interest for deep ρ^0 electroproduction). This cut defines the minimum θ_e to be $\sim$20°, which is already greater than the minimum acceptance angle of the electromagnetic calorimeters in CLAS (8°). Therefore the increase in acceptance, observed between figures 1 and 2, is due to the detection of a particle (or particles) other than the scattered electron.

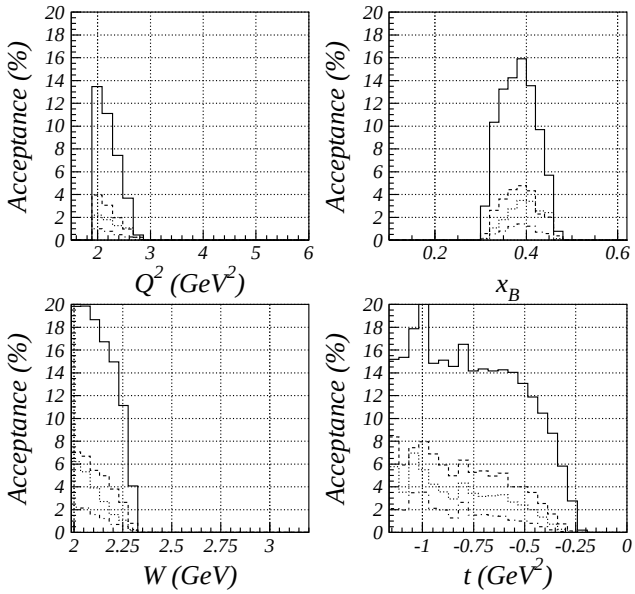

Figure 4: *As figure 1, for E_0=4 GeV.*

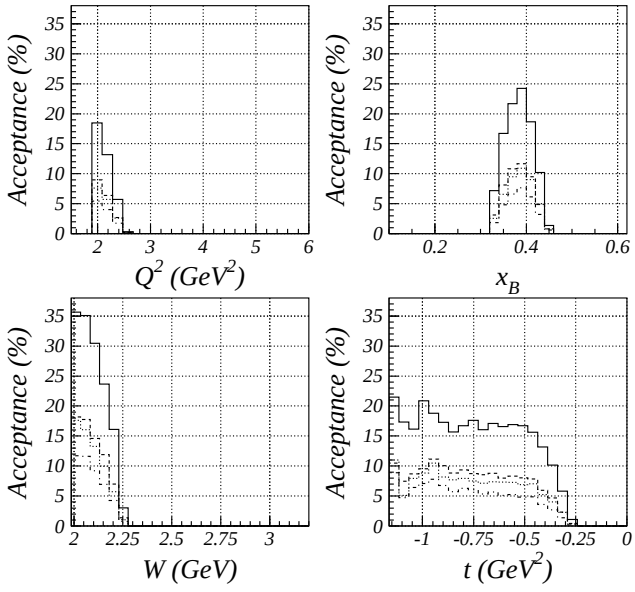

Figure 5: *As figure 1, with the target displaced upstream by 1 m and for E_0=4 GeV.*

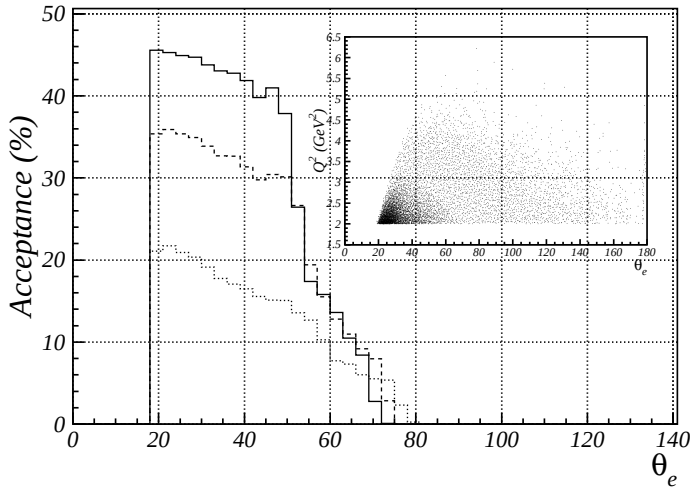

Figure 6: *The acceptance as a function of the scattered electron angle, in the laboratory frame, for the coincidence condition $e^- + p + \pi^+$. The full, dashed and dotted histograms represent the target positions of 1, 0.5 and 0 m upstream of the nominal position, respectively. This shows that the increase in acceptance is not related to a change in the minimum scattering angle. The inset shows Q^2 v's θ_e for generated events. Events with Q^2 <2 GeV^2 were rejected.*

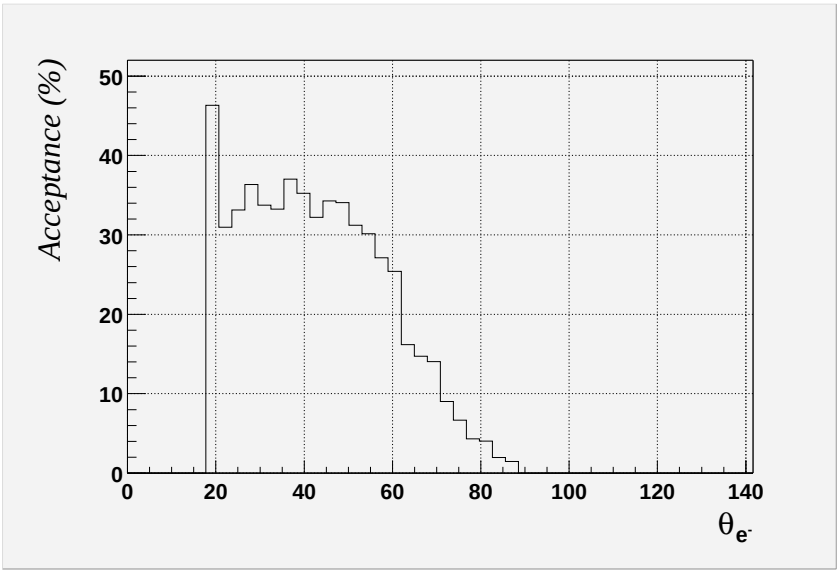

Figure 7: *As figure 6, results from GSIM simulations for the target placed at the nominal position only.*

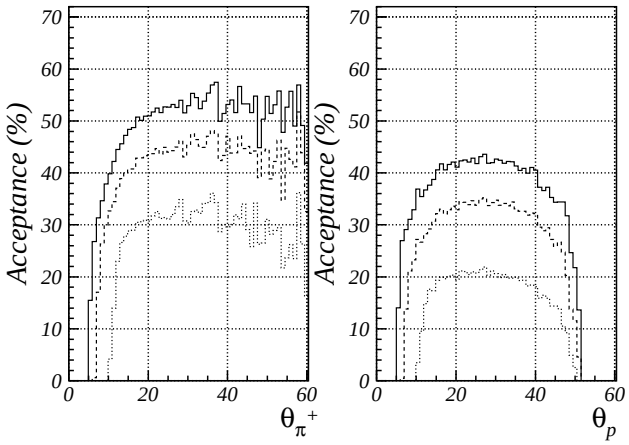

Figure 8: *The acceptance as a function of θ_{π^+} (left panel) and θ_p (right panel), for the criterion $e^- + p + \pi^+$. The full, dashed and dotted histograms represent the target positions of 1, 0.5 and 0 m upstream of the nominal position, respectively.*

Figure 8 shows the distributions of θ_{π^+} and θ_p, again with the target at 1, 0.5 and 0 m upstream of the nominal target position. It can be seen that the minimum accepted angle decreases, from $\sim$10° to $\sim$5°, for both variables when the target is moved by 1 m. (The results from GSIM are shown in figure 9 for these 2 variables with the target at nominal position only and a reasonable agreement is obtained; for FASTMC at θ_{π^-}=20° the acceptance$\simeq$30% and for GSIM at θ_{π^-}=20° the acceptance$\simeq$40%.) The count rate is highest at the forward pion angles (or low t, see figure 10). Therefore the decrease in minimum detection angle for these particles explains the significant increase in the overall acceptance.

3 Magnetic Field Strength

This section shows the effect of altering the strength of the toroidal magnetic field on the acceptances. It was envisaged that a B field lower than maximum, which would bend the reaction products less, may allow a larger acceptance for negatively charged pions at forward angles. The acceptance at forward angles is most important because of the larger count rate of pions there.

First, looking at the condition which gave most acceptance in section 2 ($e^- + p + \pi^+$), figure 11 shows that the integrated acceptances as a function of Q^2, W, θ_{π^+} and t drop by $\sim$5 % when the field strength is reduced to half its maximum. Also, the acceptance drops further when the field is reduced further. This drop in acceptance corresponds mainly to the loss of large angle scattered electrons, as can be seen from figure 12.

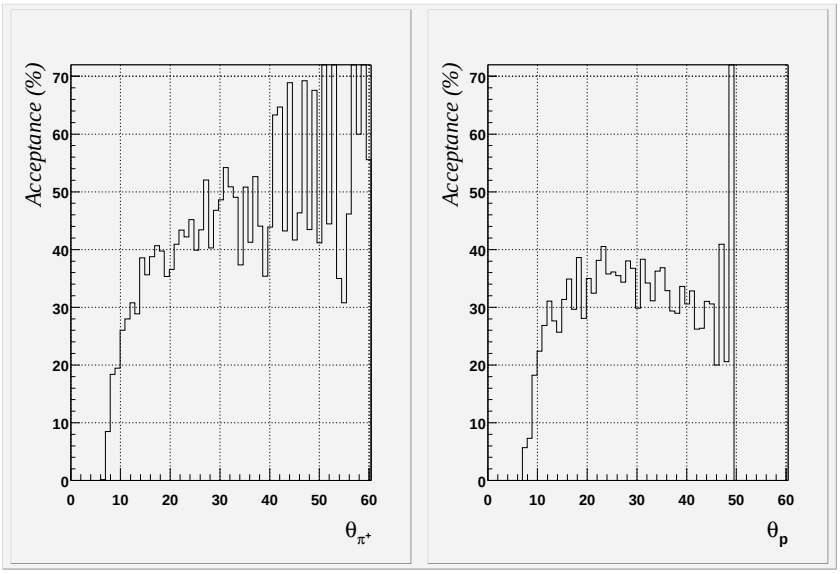

Figure 9: *As figure 8, results from GSIM simulations for the target placed at the nominal position only.*

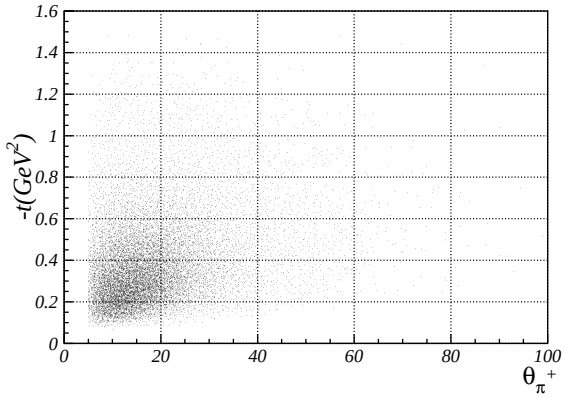

Figure 10: *The dependence of $\theta_{\pi+}$ on t, for the criterion $e^- + p + \pi^+$.*

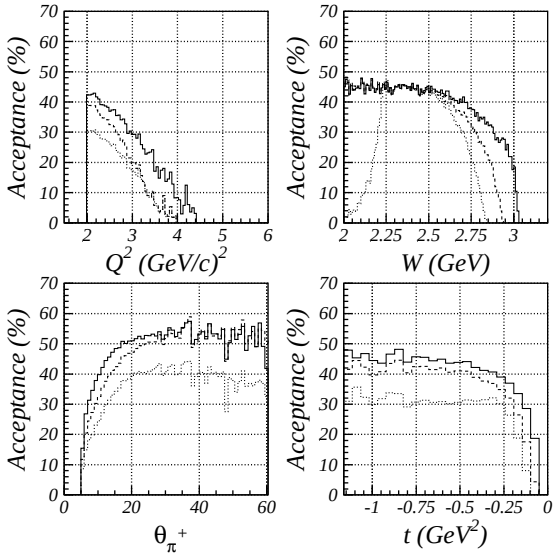

Figure 11: *Acceptance as a function of Q^2, W, $\theta_{\pi+}$ and t for the coincidence condition $e^- + p + \pi^+$. The target has been placed 1 m upstream of the nominal position. The full, dashed and dotted histograms represent the magnetic field of CLAS at full, 1/2 and 1/4 values of the maximum strength, respectively.*

For the sake of completion we have also investigated the case of the condition $e^- + p + \pi^-$. The acceptance does increase for the 1/2 strength B field, although it does not become higher than for the $e^-+p+\pi^+$ condition. Figure 13 shows the acceptance for this condition as a function of θ_{π^-} (upper left panel) and θ_e (upper right panel). The acceptance for θ_{π^-} is affected most at angles larger than 40°. The lesser bending of electrons in the half strength magnetic field causes a sharper drop in the acceptance, as a function of θ_e, at around 45°. This is again due to the electrons moving outside of the acceptance of the electromagnetic calorimeter, as discussed in the previous paragraph. The increased acceptance at lower θ_e corresponds to an increased acceptance at lower Q^2 (lower panel of figure 13). This, however, would provide no gain for the current study, as the region of interest is at high Q^2.

In conclusion, lowering the B field of CLAS indeed benefits the acceptance if the π^- is included in the criteria for an event. However, even with this benefit, it does not compare to the $e^- + p + \pi^+$ criterion (see figure 11a, Q^2=2 GeV^2, acceptance=40 % and figure 13c, Q^2=2 GeV^2, acceptance=25 %). Even by retaining the $e^- + p + \pi^-$ criterion the benefit is only apparent at low values of Q^2, which is not the region of interest in this experiment. Since the acceptance is still higher for the $e^- + p + \pi^+$ condition with full B field, this setup should be used.

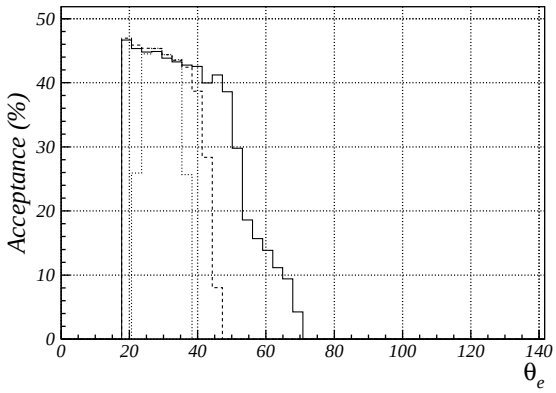

Figure 12: *Acceptance as a function of θ_e for the coincidence condition $e^- + p + \pi^+$. The target has been placed 1 m upstream of the nominal position. The full, dashed and dotted histograms represent the magnetic field of CLAS at full, 1/2 and 1/4 values of the maximum strength, respectively.*

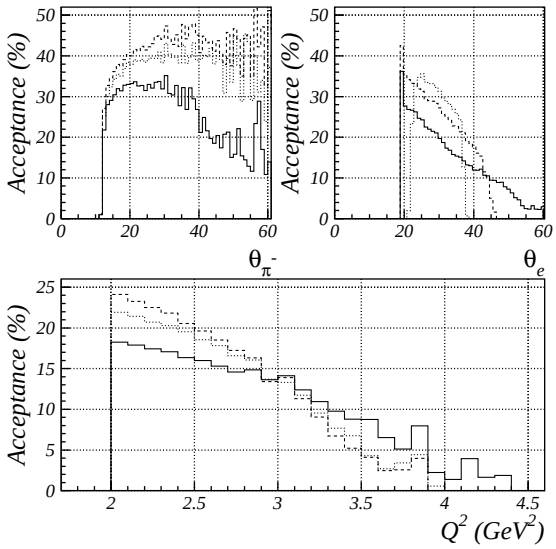

Figure 13: *The acceptance as a function of θ_{π^-} (upper left panel), θ_e (upper right panel) and Q^2 (lower panel), for the criterion $e^- + p + \pi^-$. The target has been placed 1 m upstream of the nominal position. The full, dashed and dotted histograms represent the magnetic field of CLAS at full, 1/2 and 1/4 values of the maximum strength, respectively.*

4 Magnetic Field Polarity

To complete this series of tests on the acceptances, a final investigation was performed by reversing the polarity of the magnetic field in CLAS with respect to its usual setting. A drop in acceptance was intuitively expected, however the test was performed for completeness. In normal use the field polarity causes the negatively charged particles (i.e. e^- and π^-) to be bent towards the beam axis. This setting causes them to be bent away from the beam axis. The acceptance plots of figure 1 were remade at full magnetic field strength (with the target at the nominal position) and are shown in figure 14. It can be seen that the

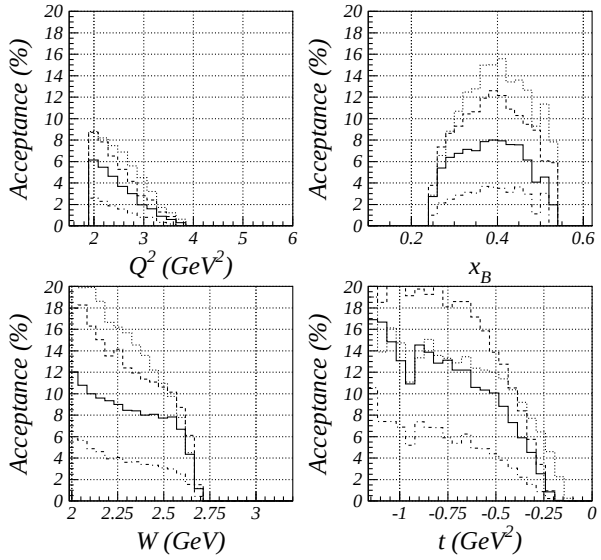

Figure 14: *As figure 1, for the magnetic field of CLAS in reverse polarity. The criteria used to define an accepted event were: Full histogram* $e^- + p + \pi^+$*, Dashed histogram* $e^- + p + \pi^-$*, Dotted histogram* $e^- + \pi^+ + \pi^-$ *and Dot–Dashed histogram* $e^- + p + \pi^+ + \pi^-$*.*

overall acceptances for all coincidence criteria drop dramatically. This result is explained by the fact that the scattered electrons are now being bent away from the beam line in the reverse polarity magnetic field. This causes most of them to be bent out of the acceptance of the electromagnetic calorimeter and affects the condition based on $e^- + p + \pi^+$ coincidences.

5 ω Production

The CLAS acceptance, for different target positions, has been similarly investigated for the omega production study ($e^- p \to e^- p \omega$ followed by $\omega \to \pi^+ \pi^- \pi^0$).

Events provided by the simulation code of Genova [3] have been filtered by the FASTMC program described above. They have been generated with the following conditions : $E_{beam} = 6\ GeV$, $1.5 \leq Q^2 \leq 6\ GeV^2$, $2 \leq W \leq 6\ GeV$ and $B = B_{max}$. In Figure 15, the Q^2, x_b, W and t acceptances are shown for different detected configurations: $ep\pi^+, ep\pi^-, e\pi^+\pi^-$ and $ep\pi^+\pi^-$. The π^0 is a priori not necessary to identify the omega channel. Therefore it has been neglected here. The detection of $ep\pi^+$ (Fig15) gives the highest acceptance as already observed for the ρ channel. Other detected configurations have a lower acceptance since they include a π^-. This particle is particularly difficult to detect with CLAS and especially for the ω channel since it has a lower momentum than in the ρ channel.

The target position has an important effect on the acceptance as can be seen on figure 16. Here, all detected channels have been summed and the Q^2 acceptance is shown for three target positions (nominal (solid line), 0.5 m upstream (dashed line) and 1m upstream (dotted line)). One observes a factor 1.7 between the nominal and the intermediate position and it goes up to a factor 2.1 for the 1 m upstream position. The integrated values presented in the Table 1 summarize the information.

Table 1: *Integrated acceptances for different Q^2 ranges and target positions, for the ω production channel. All detected configurations are included.*

	$Q^2 > 1.5$	$Q^2 > 2$	$Q^2 > 3$
z_{tgt} = 0	0.21	0.21	0.17
z_{tgt} = - 0.5 m	0.37	0.35	0.28
z_{tgt} = - 1.0 m	0.47	0.44	0.35

The acceptances have also been studied according to the strength and the polarity of the magnetic field and the beam energy. Changes observed for the ω channel are roughly the same as for the ρ channel.

6 Conclusion

In conclusion this study shows, that based on the result of FASTMC simulations (where rough agreement with GSIM has been checked, for the target at the nominal position), a significant increase in acceptance (approx. a factor of 2), would be achieved for the production of ρ and ω mesons, by displacing the target upstream of the nominal position by 1 m. No advantage is seen in using a toroidal B field lower than the maximum strength, or by reversing its polarity. The advantages of moving the target must be weighed against the difficulties in reconstructing events measured with the CLAS detector in this configuration.

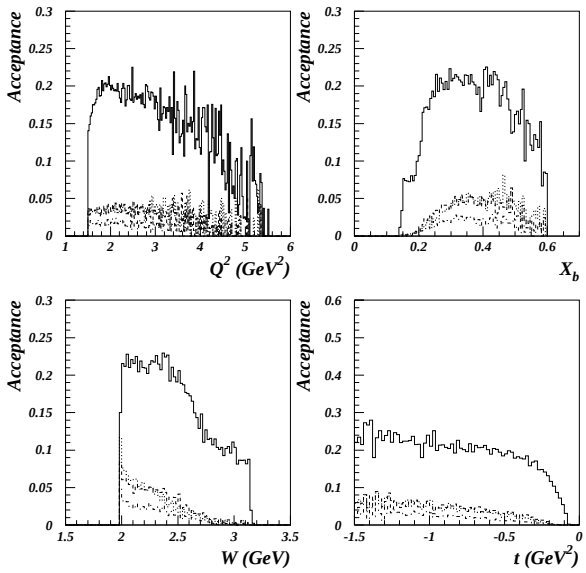

Figure 15: *The acceptance as a function of Q^2, x_b, W and t for the ω production channel, for different coincidence conditions : $ep\pi^+$ (full line), $ep\pi^-$ (dashed line), $e\pi^+\pi^-$ (dotted line) and $ep\pi^+\pi^-$ (dashed-dotted line).*

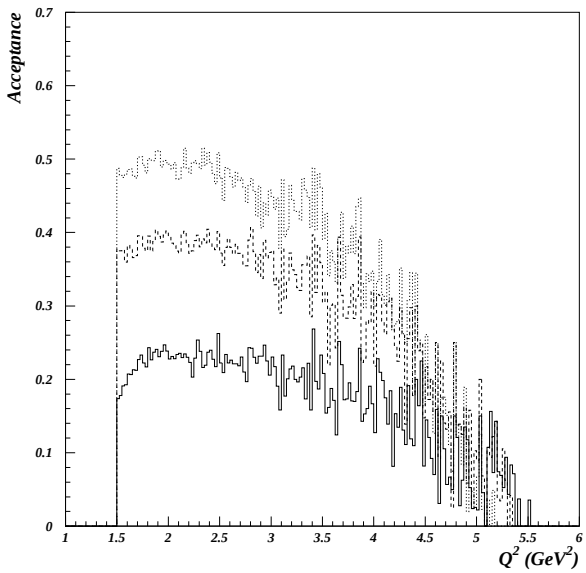

Figure 16: *The cumulated acceptance as a function of Q^2 for the ω production channel. Results are shown for the target at the nominal position (full line), the 0.5 m upstream position (dashed line) and the 1 m upstream position (dotted line).*

References

[1] E.S. Smith, "Fast Monte Carlo Program for the CLAS Detector", CLAS–Note 90–003, Feb 1990.

[2] M. Morlet, J. Van de Wiele and M. Guidal, Private Communication.

[3] M. Ripani, Private Communication.

[4] Cebaf experiment E99–105, spokespersons M. Guidal, M. Garçon and E. Smith.

[5] Elliott Wolin, GSIM User's Guide, April 1996.